WILEY-VCH

Edited by Stephen T. Liddle

Molecular Metal-Metal Bonds

Compounds, Synthesis, Properties

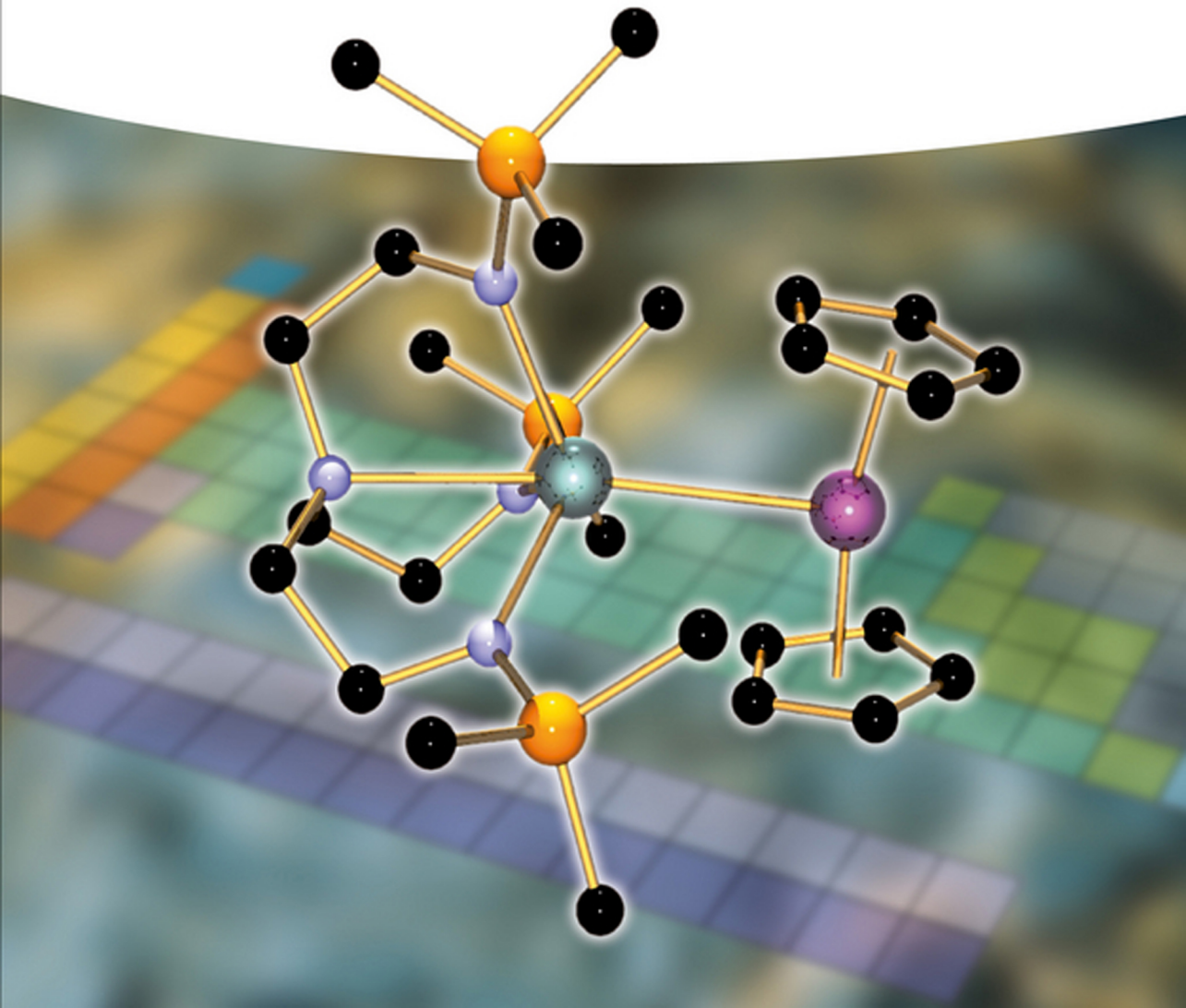

Edited by
Stephen T. Liddle

Molecular Metal–Metal Bonds

Related Titles

Frenking, G., Shaik, S. (eds.)

The Chemical Bond
Chemical Bonding Across the Periodic Table

2014
Print ISBN: 978-3-527-33315-8;
also available in electronic formats

Frenking, G., Shaik, S. (eds.)

The Chemical Bond
Fundamental Aspects of Chemical Bonding

2014
Print ISBN: 978-3-527-33314-1;
also available in electronic formats

Crabtree, R.H.

The Organometallic Chemistry of the Main Group Metals

2011
Print ISBN: 978-0-471-18431-7;
also available in electronic formats

Edited by
Stephen T. Liddle

Molecular Metal–Metal Bonds

Compounds, Synthesis, Properties

WILEY-VCH
Verlag GmbH & Co. KGaA

The Editor

Prof. Dr. Stephen T. Liddle
University of Nottingham
School of Chemistry
University Park
Nottingham, NG7 2RD
UK

Library of Congress Card No.: applied for

British Library Cataloguing-in-Publication Data
A catalogue record for this book is available from the British Library.

Bibliographic information published by the Deutsche Nationalbibliothek
The Deutsche Nationalbibliothek lists this publication in the Deutsche Nationalbibliografie; detailed bibliographic data are available on the Internet at <http://dnb.d-nb.de>.

Print ISBN: 978-3-527-33541-1
ePDF ISBN: 978-3-527-67338-4
ePub ISBN: 978-3-527-67337-7
Mobi ISBN: 978-3-527-67336-0
oBook ISBN: 978-3-527-67335-3

Cover Design Grafik-Design Schulz, Fußgönheim, Germany
Typesetting Laserwords Private Limited, Chennai, India
Printing and Binding Markono Print Media Pte Ltd, Singapore

Printed on acid-free paper

To previous and current co-workers.

Contents

Preface

When Wiley-VCH approached me with the suggestion that I edit a textbook on metal–metal complexes, I was, at first, not convinced. Published in 2005 and already in its third edition, *Multiple Bonds Between Metal Atoms,* edited by F. Albert Cotton, Carlos A. Murillo, and Richard A. Walton, presents a comprehensive treatment of the area. However, time moves on, and so does science. Many advances have occurred in the intervening decade, and some entirely new areas of metal–metal chemistry have emerged while old ones have been reinvigorated. It was felt that a textbook to update the area was warranted and that its scope had to encompass the newfound breadth as well as depth of the area. Thus, the decision was made to cover all areas of the Periodic Table rather than just the d-block. This then raises the question of the structure of the book. Do we cover by group number? Do we cover by ligand class? Do we cover by structural motif? The options are varied, and each has its pedagogical advantages and disadvantages. In the end, the decision was made to generally treat each class by group number with the exception that s-block metal–metal bonds could be covered in one chapter. The result is a book of 15 chapters, which starts with a general overview of metal–metal bonding before dealing with individual groups.

In every chapter, authors have endeavored to be as comprehensive as possible, although an encyclopedic treatment is simply not possible due to the sheer volume of the literature and so a balance had to be struck. The authors have attempted to highlight important compounds and demonstrate important concepts and reactions. Inevitably the level of attention varies between areas and we apologize in advance for the inadvertent omission if the reader cannot find their favorite compound. Each chapter mentions important molecules at the genesis of each area but focuses principally on research published since 2005 as repetition of the above-mentioned treatise would be pointless. While attempts were made to harmonize the general structure of chapters, it had to be recognized that each area has its own specialties and by retaining individual author styles each chapter remains fresh to the reader. This approach has resulted in some duplications, but it is felt that this provides the reader with more than one perspective of a given area and thus provides the pedagogically useful comparisons that are to some extent lost when categorizing metal–metal compounds by group numbers.

To produce a book in this area with the necessary breadth and depth is a formidable challenge for anyone, and in order to achieve this feat in any reasonable timescale, to not render the book obsolete before it is published, it was necessary to call on the help of others. This book project has been very fortunate that a number of authors have enthusiastically answered the call to arms. They vary from rising stars to established leaders of their fields, but importantly are all experts and have written from positions of authority. One particularly pleasing aspect is that several authors from *Multiple Bonds Between Metal Atoms* have found the time to contribute to this book, thus providing a link from what has gone before to now. I wish to take this opportunity to thank all the authors for their invaluable contributions and the editorial staff at Wiley-VCH for their patience.

University of Nottingham, UK
March 2015

Stephen T. Liddle

List of Contributors

Joseph A.B. Abdalla
University of Oxford
Department of Chemistry
Chemistry Research Laboratory
Mansfield Road
Oxford OX1 3TA
UK

Simon Aldridge
University of Oxford
Department of Chemistry
Chemistry Research Laboratory
Mansfield Road
Oxford OX1 3TA
UK

Jitendra K. Bera
Indian Institute of Technology Kanpur
Department of Chemistry
Kanpur 208016
India

Matthew P. Blake
University of Oxford
Department of Chemistry
Chemistry Research Laboratory
Mansfield Road
Oxford OX1 3TA
UK

Helen T. Chifotides
Texas A&M University
Department of Chemistry
College Station
TX 77843
USA

Malcolm H. Chisholm
The Ohio State University
Department of Chemistry and
Biochemistry
Columbus, 100 W. 18th Avenue
OH 43210
USA

Kim R. Dunbar
Texas A&M University
Department of Chemistry
College Station
TX 77843
USA

François P. Gabbaï
Texas A&M University
Department of Chemistry
Ross street, College Station
TX 77843
USA

Lutz H. Gade
Anorganisch-Chemisches Institut der
Universität Heidelberg
Lehrstuhl für Anorganische Chemie III
Im Neuenheimer Feld 270
69120 Heidelberg
Germany

Sundargopal Ghosh
Indian Institute of Technology Madras
Department of Chemistry
Sardar Patel Road
Chennai 600036
Tamil Nadu
India

Thomas G. Gray
Case Western Reserve University
Department of Chemistry
10900 Euclid Avenue
Cleveland, OH, 44106
USA

Sjoerd Harder
Universität Erlangen-Nürnberg
Lehrstuhl für Anorganische und
Metallorganische Chemie
Egerlandstrasse 1
91058 Erlangen
Germany

Cameron Jones
Monash University
School of Chemistry
PO Box 23
Wellington Road
Melbourne 3800
Australia

James S. Jones
Texas A&M University
Department of Chemistry
Ross street, College Station
TX 77843
USA

Rhett Kempe
Universität Bayreuth
Lehrstuhl Anorganische Chemie II
95440 Bayreuth
Germany

Robert J. Less
Cambridge University
Chemistry Department
Lensfield Road
Cambridge CB2 1EW
UK

Stephen T. Liddle
University of Nottingham
School of Chemistry
University Park
Nottingham NG7 2RD
UK

Connie C. Lu
University of Minnesota
Department of Chemistry
Twin Cities
Minneapolis, 55455 MN
USA

Erli Lu
University of Nottingham
School of Chemistry
University Park
Nottingham NG7 2RD
UK

John E. McGrady
University of Oxford
Physical and Theoretical Chemistry
Laboratory
South Parks Road
Oxford OX1 3QZ
UK

Philip Mountford
University of Oxford
Department of Chemistry
Chemistry Research Laboratory
Mansfield Road
Oxford OX1 3TA
UK

Benjamin Oelkers
Technische Universität Kaiserslautern
Fachbereich Chemie
Erwin-Schrödinger-Str. 54
67663 Kaiserslautern
Germany

Baofei Pan
Texas A&M University
Department of Chemistry
Ross street, College Station
TX 77843
USA

Nathan J. Patmore
University of Huddersfield
Department of Chemical Sciences
Queensgate
Huddersfield HD1 3DH
UK

Frederic Poineau
University of Nevada Las Vegas
Department of Chemistry
Maryland Parkway
Las Vegas, NV 89154
USA

Dipak Kumar Roy
Indian Institute of Technology Madras
Department of Chemistry
Sardar Patel Road
Chennai 600036
Tamil Nadu
India

Joseph P. Sadighi
Georgia Institute of Technology
Chemistry and Biochemistry
901 Atlantic Drive
Atlanta, GA 30332-0400
USA

Biswajit Saha
Indian Institute of Technology Kanpur
Department of Chemistry
Kanpur 208016
India

Alfred P. Sattelberger
Argonne National Laboratory
9700 South Cass Avenue
Lemont, IL 60439
USA

Andreas Stasch
Monash University
School of Chemistry
PO Box 23
Wellington Road
Melbourne 3800
Australia

Stephen J. Tereniak
University of Minnesota
Department of Chemistry
Twin Cities
Minneapolis, MN
USA

Dominic S. Wright
Cambridge University
Chemistry Department
Lensfield Road
Cambridge CB2 1EW
UK

Xian Wu
Universität Erlangen-Nürnberg
Lehrstuhl für Anorganische und
Metallorganische Chemie
Egerlandstrasse 1
91058 Erlangen
Germany

1
Introduction and General Survey of Metal–Metal Bonds

John E. McGrady

1.1
Introduction

The interactions between metal ions continue to challenge our understanding of the nature of the chemical bond. The first decade of the new millennium has been a particularly productive period, with a number of landmark discoveries including the ultrashort Cr^{I}–Cr^{I} bonds [1], the Mg^{I}–Mg^{I} and Zn^{I}–Zn^{I} dimers of Jones [2] and Carmona [3], respectively, and the distannynes [4] and diplumbynes [5], the heavier analogs of acetylene. Moreover, metal–metal bonded systems are increasingly finding applications in fields as diverse as molecular electronics [6], organometallic catalysis [7], and even in enzyme-mediated transformations [8]. The pioneering work in the field dates back almost exactly half a century and is inevitably associated with Cotton and the quadruple bond in $[Re_2Cl_8]^{2-}$ [9–11]. Since that time, the three transition series have proved the most fertile source of metal–metal bonds, largely because the presence of (n + 1)s, (n + 1)p, and nd orbitals in the valence region offers an unrivaled potential for strong interactions. Nevertheless, the transition metals make up fewer than half of the know "metallic" elements, and metal–metal bonds in discrete molecular systems are becoming increasingly well established for the s-, p-, and even the f-block elements [12].

In general, the formation of bonds between metals is a delicate balancing act: on the one hand the valence orbitals involved must be sufficiently diffuse to afford substantial diatomic overlap, on the other, competitive binding of additional ligands must be avoided. In fact, much of the recent progress in the field has come through the elegant design of sterically encumbered ligands that block access of additional ligands to the metal coordination sphere. The intrinsic strength of the bond between two metals depends on many factors, including the number of available electrons and the radial and angular properties of the valence orbitals involved. The angular properties determine the local symmetry of the overlap between metal-based orbitals: σ, π, δ, the latter being unique to systems with valence orbitals with $l > 1$ (i.e., d or f orbitals, Figure 1.1). While undoubtedly iconic in the context of metal–metal interactions, δ bonding is typically very weak and the components with σ and π symmetry dominate the overall bond strength. The radial properties of the orbitals control many of the important periodic trends: radial distribution functions for the valence orbitals in exemplary s-, p-, d-, and f-block elements (Mg, Sn, Cr, and Eu, respectively) are collected in Figure 1.2. In the main groups, the valence ns and/or np orbitals are generally well extended relative to core orbitals and so the equilibrium geometry affords near-optimal overlap. The more diffuse nature of orbitals with higher principal quantum number then leads to reduced overlap and hence to relatively weaker bonds in the heavier members of the group: the multiple bonds in distannenes and distannynes are classic examples. The inert-pair effect also means that metal–metal bonding in the heavier post transition metals is increasingly dominated by np orbitals, the ns character accumulating in nonbonding lone pairs. In the transition series (exemplified by Cr in Figure 1.2), in contrast, the radial maxima of the valence nd orbitals lie in the same region as those of the filled ns and np core, and so diatomic overlap is intrinsically small. In this case, an increase in principal quantum causes a greater fraction of the

Molecular Metal-Metal Bonds: Compounds, Synthesis, Properties, First Edition.
Edited by Stephen T. Liddle.

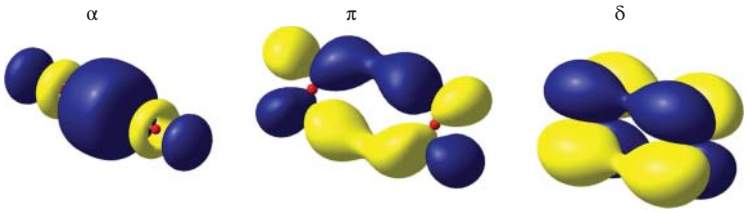

Figure 1.1 σ, π, and δ overlap of d orbitals between two arbitrary metal centers.

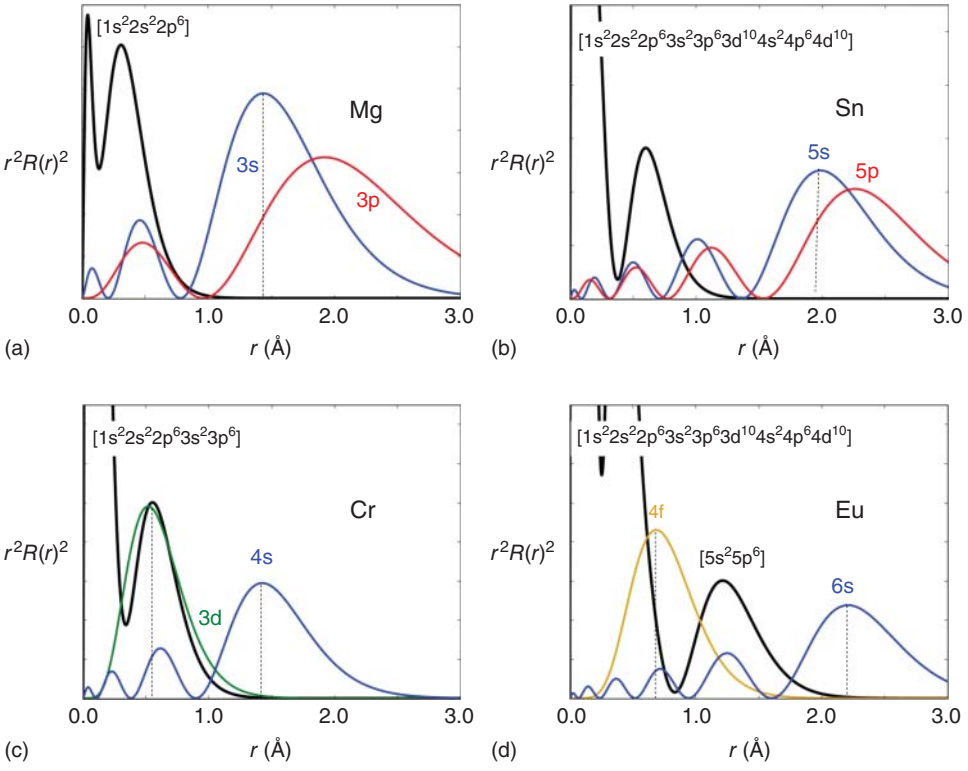

Figure 1.2 Radial distribution functions of the valence orbitals in the (a) s-(Mg), (b) p-(Sn), (c) d-(Cr), and (d) f-(Eu) blocks of the periodic table. Black lines correspond to the core density.

nd orbital to protrude outside the core and so d-d overlap increases, rather than decreases, down a group. The trend in bond strengths is therefore precisely the opposite of that in the main group: metal–metal bonding becomes stronger in the heavier transition metal elements. The lanthanide and actinide series (Eu in Figure 1.2.) can be regarded as extreme versions of the transition elements, with the nf orbitals now lying almost entirely inside the radial maxima of filled (n + 1)s and (n + 1)p and unavailable to participate in effective bonding interactions.

It is important to emphasize from the outset that metal–metal bonds present a substantial challenge to electronic structure theory, particularly where diatomic overlap is weak and the electrons are highly correlated. The chromium dimer, Cr_2, for example, is a notoriously difficult case and has been the subject of debate for decades [13]. Some progress toward a quantitative understanding of these correlation effects has been made through Complete Active Space Self Consistent Field (CASSCF) and related wavefunction-based techniques, but much of our qualitative understanding

of metal–metal bond remains based on single determinant methods. While such methods are necessarily deficient in the limit of weak overlap, they have the considerable advantage of affording a transparent molecular orbital–based picture. Density functional theory (DFT) is the tool of choice in most modern research laboratories, but the early contributions made using Extended Hückel theory, most notably by the Hoffmann school, should be acknowledged [14]. The emphasis in this introduction is firmly on qualitative overlap arguments that have, typically, followed hard on the heels of the synthesis of new types of compound. The coverage reflects the structure of the periodic table, with metal–metal bonds mediated primarily by s orbitals discussed first, followed by the d, f, and p blocks. The purpose of this introductory chapter is to provide a periodic framework for the discussion of specific classes of metal–metal bonds that appear in subsequent chapters.

1.2
Metal–Metal Bonds Involving *s* Orbitals

The chemistry of groups 1 and 2 is characterized almost exclusively by the +1 and +2 oxidation states, respectively, leaving little scope for direct covalent interactions between the metals. Exceptions occur in the relatively electronegative lighter elements, Li and Be, where the occupied bonding orbitals carry substantial metallic character. A textbook case is the electron-deficient Li_4Me_4 tetramer, where the bonding orbitals have both Li–Li and Li–C bonding character and the Li–Li distance is rather short at 2.56 Å [15]. Examples of unsupported metal–metal bonds in subvalent Mg^I species emerged only in the 1980s when species such as HMg–MgH and ClMg–MgCl were characterized in inert matrices [16]. The first species containing direct Mg^I–Mg^I bonds (Mg–Mg = 2.8508(12), 2.8457(8) Å) to be isolated were reported only in 2007 by Jones and Stasch (Figure 1.3) [2]. The Mg–Mg bonding is dominated by the Mg 3s orbital (>90%), with homolytic bond dissociation energies in the region of ~45 kcal mol^{-1}. The radial disparity between the very diffuse 3s valence orbital and a relatively compact [$1s^2 2s^2 2p^6$] core (shown in Figure 1.2) means that the electron density in the bond is somewhat isolated from the nuclei [17–19], and these dimers are very effective two-electron reducing agents [20].

The potential for extending this chemistry to heavier members of group 2 seems rather limited, primarily because the high energy of the ns orbitals makes the interception of the M^I oxidation state increasingly challenging. Moreover, the radial maxima become even more diffuse, making the putative M–M bonds very weak. For example, Ca–Ca bonds have been computed to be almost 1 Å longer than their Mg counterparts, with bond dissociation energies lowered by 50% [21]. On the opposite side of the first transition series in group 12, however, penetration through the nd^{10} core stabilizes the (n + 1)s orbital and contracts its radial maximum, making bonds mediated by the s orbitals accessible once again. Prior to 2004, the chemistry of Zn–Zn bonded species was limited to reports of the Zn_2^{2+} cation in $Zn/ZnCl_2$ melts [22] and the spectroscopic characterization of the dihydride HZn–ZnH in inert matrices [23]. Carmona's report of the structure of dizincocene (Cp*Zn–ZnCp*), with a Zn–Zn separation of 2.3050(3) Å and two parallel Cp* rings, represents the first structurally characterized example of its kind (Figure 1.3) [3]. The nature of the Zn–Zn bond in Zn_2^{2+} and related species had been extensively discussed well before Carmona's seminal discovery [24], but the realization that Cp*Zn–ZnCp* was a stable chemical entity prompted a number of theoretical investigations [25]. Much like the Mg–Mg bond, the Zn–Zn bond in dizincocene is mediated primarily by overlap of the s orbitals (4s in this case), which make up ~90% of the character of the HOMO: symmetry allowed mixing with the p_z and d_{z^2} orbitals is minimal [26]. Compared to the Mg–Mg bonds, however, the contraction of the 4s orbital leads to much shorter and stronger (65 kcal mol^{-1} vs 45 kcal mol^{-1}) bonds. Numerous other Zn–Zn bonded species have emerged in the decade since Carmona's report, primarily with chelating nitrogen-based ligands [27], and these compounds have even found use as reagents in chemical synthesis [28]. The nature of the Zn–Zn bonding appears to be relatively similar

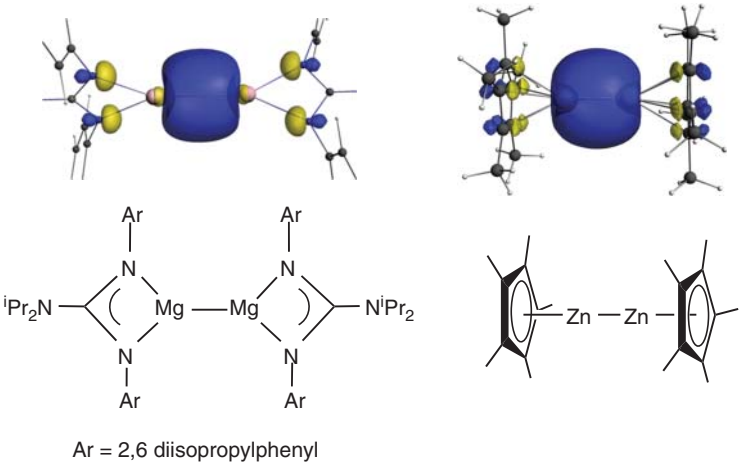

Figure 1.3 HOMOs of ((Ar)NC(N^{i}Pr$_2$)N(Ar))Mg–Mg((Ar)NC(N^{i}Pr$_2$)N(Ar)) and Cp*Zn–ZnCp*.

in all cases, although linear coordination to a strong σ-donor ligand in ArZn–ZnAr (Ar = C_6H_3-2,6-(C_6H_3-2,6-^{i}Pr$_2$)$_2$) [29] results in a somewhat longer Zn–Zn bond (2.3591(9) Å) with more extensive s/p$_z$ mixing, the latter making up ~30% of the Zn character in the HOMO.

The heavier dications Cd_2^{2+} and Hg_2^{2+} are relatively common structural motifs in both the solid state and melts [30], but discrete molecular analogs of the Zn–Zn bonded systems are scarce because coordination of ligands tends to induce disproportionation to M^0 and M^{II}. In fact, the first structurally characterized complex of Hg_2^{2+}, the silyl complex $Hg_2[Si(SiMe_2SiMe_3)_3]_2$ with an Hg–Hg separation of 2.6569(1) Å, was described only in 1999 [31]. Alongside ArZn–ZnAr, the Cd–Cd [32] and Hg–Hg [33] analogue presented the first opportunity to compare trends in bonding down group 12 within an isostructural series. The Cd–Cd bond appears to be rather similar to the Zn–Zn analog, with dominant 5s character mixed with some 5p$_z$. In the mercury congener, however, relativistic stabilization of the 6s orbital reduces the 5d$_{z^2}$/6s separation, and ~5% d$_{z^2}$ character is present in the Hg–Hg bonding HOMO. In conjunction with the lanthanide contraction, the result is that the Hg–Hg bond (2.5738(3) Å) is marginally shorter than its Cd–Cd analog (2.6257(5) Å) despite the presence of 32 extra electrons in the core shells.

The predominance of the +3 oxidation state in aluminum chemistry means that, like the group 1, 2, and 12 analogs, homometallic covalent Al–Al bonds are relatively scarce. A number of subvalent Al^I and Al^{II} species have, however, been synthesized, including the first molecular Al–Al bond in $Al_2(CH(SiMe_3)_2)_4$ (Al–Al = 2.660(1) Å) [34]. Even lower oxidation states of Al are generally stabilized through the formation of pseudo-spherical clusters such as the tetrahedral Al^I species, $Cp^*_4Al_4$ [35] and the remarkable icosahedral "superhalide" ion, $[Al_{13}]^-$ [36]. The latter is observed in gas-phase experiments, where it is notably resistant to reaction with oxygen compared to neighboring members of the $[Al_n]^-$ series. The stability of the $[Al_{13}]^-$ cluster can be understood using a delocalized "jellium" model, where the 40 valence electrons are confined in an approximately spherical positive potential generated by the nuclei and the core 1s, 2s and 2p electrons (Figure 1.4). The degeneracies in the energy level ordering shown in Figure 1.4 ($1a_{1g} < 1t_{1u} < 1h_g < 2a_{1g} < 2t_{1u} < 1g_u = 1t_{2u} < 2h_g$) are reminiscent of a superatomic ordering sequence 1s < 1p < 1d < 2s < 2p < 1f < 2d, reflecting the approximate spherical symmetry of the confining potential.

In contrast to the now relatively extensive metal–metal bonded chemistry of subvalent Mg, Al, and Zn, homometallic bonds involving the 6s and 7s orbitals of the lanthanide and actinides elements are rare (diatomic overlap between the 5f orbitals in U_2 and other cases is discussed later). Their absence is largely a consequence of the relatively low second and third ionization energies (compared to Al), which reduce the stability of the +1 and +2 oxidation states. Examples

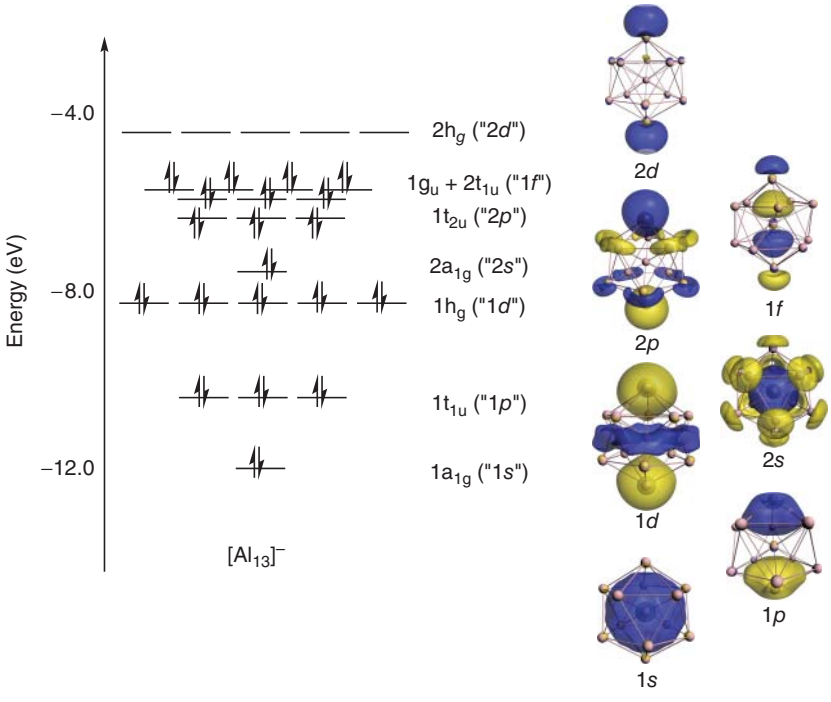

Figure 1.4 The icosahedral $[Al_{13}]^-$ cluster: a "superhalide."

of metal–metal bonds are limited to heterobimetallic cases where the lanthanide acts as a Lewis acid in combination with strongly Lewis basic transition metal fragments such as $[Fe(CO)_4]^{2-}$ or $[Ru(Cp)(CO)_2]^-$. In $(Cp)_2Lu(thf)$-$Ru(Cp)(CO)_2$, for example, the interaction between the metals is primarily electrostatic (Lu–Ru 2.995(2) Å) [37], the HOMO having <10% Lu character. A similar electrostatic picture emerges even in adducts of the earlier lanthanide ions such as Nd^{III}, where the f shell is higher in energy and only partly filled [38]. The more diffuse 5f orbitals of the actinides allow higher oxidation states to be accessed and, in principle, also allow the f orbitals to participate directly in the bonding. Substantial charge transfer from an $Al(\eta^5\text{-}C_5Me_5)$ unit to U^{III} has been reported in $(\eta^5\text{-}C_5H_4\text{–}SiMe_3)_3U\text{–}Al(\eta^5\text{-}C_5Me_5)$ [39], and there is even some evidence for weak π overlap involving the 5f orbitals in the U–Re bond in $[\{N(CH_2CH_2NSiMe_3)_3\}URe(\eta^5\text{-}C_5H_5)_2]$ and the U–Ga bond in $[(Tren^{TMS})U\{Ga(NArCH_2)_2\}(THF)]$ [40]. The role of the 5f orbitals is, however, a relatively minor component of the bonding in all cases.

1.3
Metal–Metal Bonds Involving d Orbitals

Over the past 50 years, the three transition series have been responsible for the vast majority of metal–metal bonded species, and an enormous number of dimers and larger clusters are now known. In addition to providing a unique insight into the nature of the chemical bond, these clusters have been exploited for their catalytic potential [7], and a biological role for a Ni–Fe bond in Ni–Fe hydrogenases has even been proposed [8]. Transition metal–metal bonds may be broadly classified into two types: "supported" bonds that have ligands that bridge the two centers and "unsupported" bonds that do not. In the supported class, the relative importance of metal–metal and metal–ligand interactions is often difficult to delineate because any single molecular orbital may feature contributions from both. On the other hand, the presence of bridging ligands confers great flexibility, simply because the

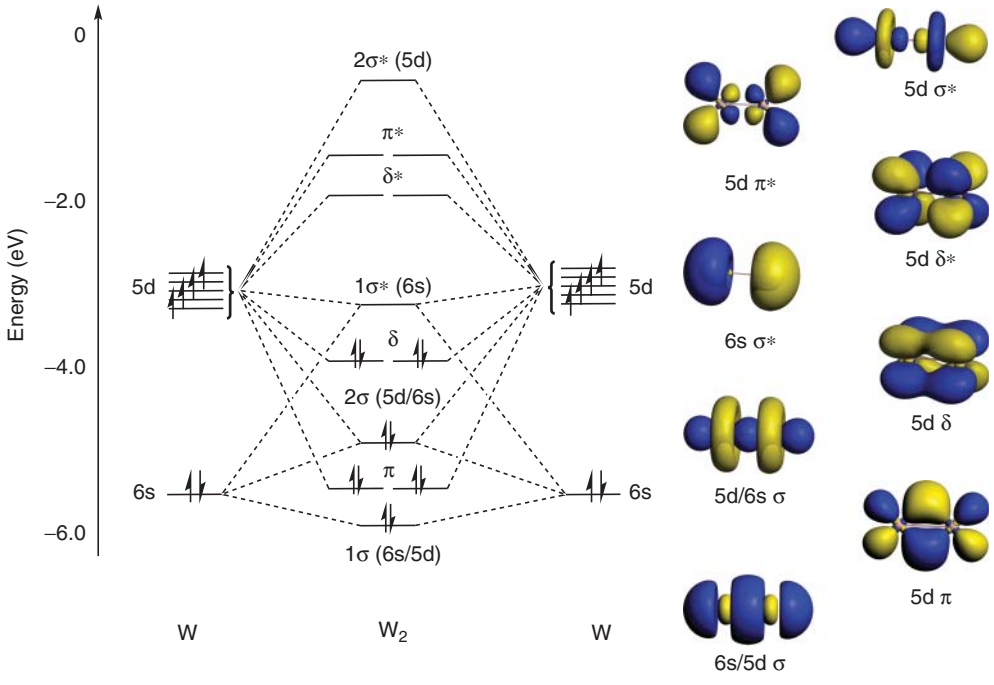

Figure 1.5 The singlet ground state of sextuply bonded W_2.

cluster does not rely solely on the metal–metal bond for its integrity. The limit of negligible direct overlap of the metal orbitals corresponds to the extensive class of exchange-coupled clusters, which lie outside the remit of this book. There are, however, a few intermediate cases where the metal–metal bond is partially formed, and even cases where distinct bonded and nonbonded isomers can be isolated [41, 42].

A survey of the electronic structure of the naked transition metal diatomics, M_2, serves to highlight many of the key periodic trends that emerge in their more chemically relevant ligated analogs. The diatomics encompass a wide range of metal–metal bond types, from strong multiple bonding to weak magnetic coupling, and they have been used as a testing ground for successive generations of theoretical methods. The elements near the center of the transition series are the most interesting from a bonding perspective as they offer the potential for extreme high bond orders, up to six in the dimers of the group VI metals Cr_2, Mo_2, and W_2. The molecular orbital array for W_2, the heaviest member of the series, illustrated in Figure 1.5 illustrates the basic features of the sextuple bond: the doubly degenerate π and δ components are supplemented by *two* distinct orbitals with σ symmetry, 1σ and 2σ, each with mixed $5d_{z^2}$/6s character. 2σ represents a conventional σ bonding orbital, in so much as the dominant $5d_{z^2}$ character is concentrated along the internuclear axis. In 1σ, in contrast, the dominant 6s character concentrates the overlap in a cylindrical region around the axis, reducing electron–electron repulsions with the 2σ component. The $5d_{z^2}$/6s hybridization is closely related to the Orgel/Dunitz mechanism used to account for the preference for linear coordination in complexes of the coinage metals [43].

The formal bond order of 6 in W_2 reflects the structure of the molecular orbital diagram but is clearly simplistic in that it fails to take into account the very different contributions of the σ, π, and δ components to the overall bond strength. In the case of the δ bonds in particular, the weak overlap leads to a small HOMO–LUMO gap, and the single determinant description of the electronic structure that is implicit in the molecular orbital diagram can be inadequate. Within the constraints of single determinant methods such as DFT, the weakness of the δ bond (and, to a lesser extent, the π

component) manifests itself in a tendency toward symmetry breaking, wherein electrons of opposite spin localize on different centers. For example, Bauschlicher's study of Cr_2 revealed net spin densities of ±2.7 at opposite centers, reflecting the strong tendency of the electrons in both the δ and π bonds to localize [44]. The potential energy surface for Cr_2 also highlights a link to the main group species discussed previously. A minimum at the equilibrium separation of 1.67 Å allows for substantial 3d–3d overlap, but a plateau is also present in the region of 2.5 Å, a result of residual overlap between the more diffuse 4s orbitals. The bonding in this region is in fact very reminiscent of that in the Mg_2^I and Zn_2^I dimers, in so much as 4s–4s overlap is the dominant feature: the three systems differ only in the size of the spherically symmetric 3d cores: d^0, d^5, and d^{10} for $Mg^I{}_2$, $Cr^0{}_2$, and $Zn^I{}_2$, respectively. Multiconfigurational character also becomes apparent in CASSCF calculations, where the effective bond orders of 5.2, 5.2, and 4.52 for W_2, Mo_2, and Cr_2, respectively, highlight the weakness of the δ component, particularly in the lightest member of group 6 [45]. In Mn_2, the five 3d electrons on each center are again weakly antiferromagnetically coupled, but both in- and out-of-phase combinations of the 4s orbital are now doubly occupied. Mn_2 can therefore be viewed as an analog of an inert gas dimer, where the bonding is dominated by van der Waals' forces, and the Mn–Mn separation in the $^1\Sigma_g^+$ ground state has been estimated at 3.64 Å [46]. Perhaps unsurprisingly this situation presents a substantial challenge to DFT, and computed Mn–Mn separations ranging from 1.6 to 3.5 Å have been reported [47].

The increasing strength of bonds involving nd orbitals down a group is a general feature of transition metal chemistry, the origins of which lie in the more diffuse nature of the 4d and 5d orbitals relative to s and p orbitals with the same principal quantum number: the greater exposure of the nd orbital *increases* diatomic d–d overlap from its very low value in the first transition series. A quantitative understanding of periodic trends, however, also requires an appreciation of the changes in electron–electron repulsion as the bond is formed. In the limit of very weak bonding (for example, as in the Mn_2 case), the individual atoms adopt local high-spin configurations, thereby minimizing electron–electron repulsions. The sharing of electron density in covalent bonds necessarily equalizes the spin densities at the two atoms, causing an increase in electron–electron repulsion. Thus, covalent bonding represents a compromise between overlap, which lowers the kinetic energy and so favors bond formation and the competing increase in electron–electron repulsions. The latter are largest in the compact 3d orbitals, and so in addition to the weak overlap, the lighter elements experience a greater increase in electron–electron repulsion upon formation of a covalent bond. A detailed analysis suggests that the two factors contribute approximately equally to the overall trend to stronger metal–metal bonds in the heavier transition elements [48, 49].

An introduction to metal–metal bonding in the transition metals would be incomplete without a discussion of the iconic quadruple bond in $[Re_2Cl_8]^{2-}$. This molecule represents a major landmark in inorganic chemistry, simply because the δ component of the bond was entirely without precedent in the main group. The quadruple bond has subsequently become synonymous with the field of metal–metal bonding, and its structure and properties have been extensively reviewed, most prominently in the seminal textbook "*Multiple Bonds Between Metal Atoms*." [50] The short Re–Re separation and eclipsed nature of the $ReCl_4$ units in an anion formulated as $[Re_2Cl_8]^{4-}$ (in "(pyH)(H)$ReCl_4$") were in fact first noted by Kuznetsov and Koz'min in 1963 [10], but a subsequent study of the potassium compound $KReCl_4.H_2O$ by Cotton and Harris revealed a dianion with an Re–Re distance of 2.241(7) Å, now correctly formulated as $[Re_2Cl_8]^{2-}$ [9]. Very soon afterward, Cotton presented the first electronic rationale for the structure [11], and the essential features of this model underpin all the more sophisticated treatments that have been reported in the subsequent half century. Cotton's model, summarized in Figure 1.6, shows how the electronic structure emerges naturally from perturbations to the diatomic developed in Figure 1.5. The combination of the high oxidation state (Re^{III}) and the square-planar ligand field removes the 6s and $5d_{x^2-y^2}$ orbitals from the valence manifold, leaving only $5d_{z^2}$, $5d_{xz}$, $5d_{yz}$, and $5d_{xy}$ available to form the Re–Re bond. The σ, π, and δ linear combinations that result from diatomic overlap give rise to a $\sigma^2\pi^4\delta^2$ ground-state configuration with a

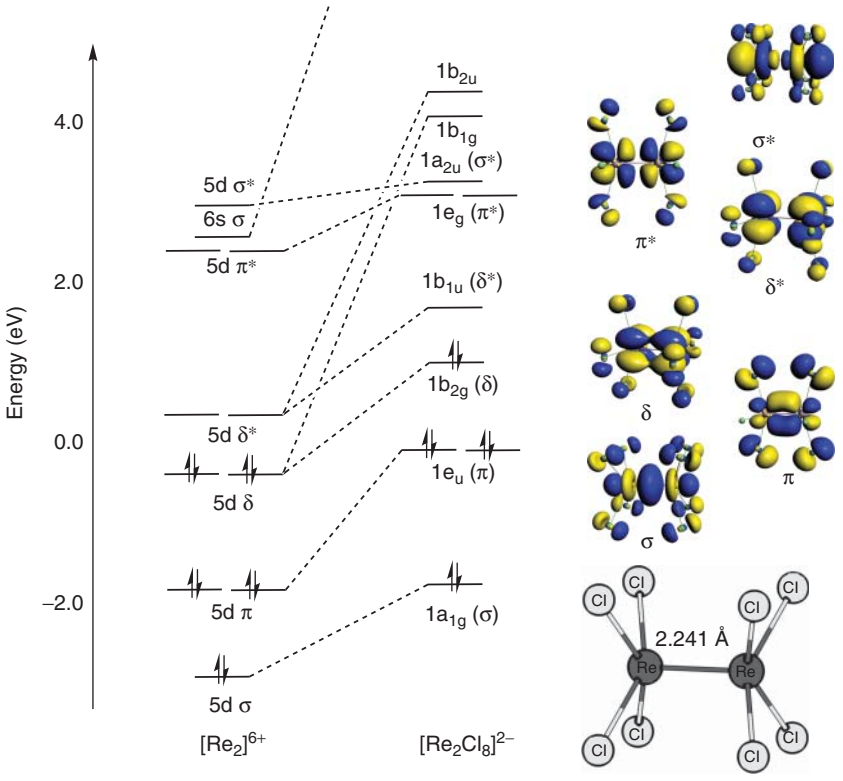

Figure 1.6 The quadruple bond in $[Re_2Cl_8]^{2-}$ (the midpoint of the δ/δ* pair is taken as an arbitrary zero of energy).

formal bond order of 4.0. The δ overlap between the d_{xy} orbitals can account for the adoption of the fully eclipsed conformation, although it has also been argued that hyperconjugation between Re–Cl σ and Re–Cl σ* orbitals contributes to the conformational preference [51].

While the basic features of Figure 1.6 were established by Cotton's 1965 paper, attempts to quantify the strength of the δ bond had to await the emergence of more sophisticated theoretical models [52]. A 1994 CASSCF calculation on $[Re_2Cl_8]^{2-}$ using an (8,8) active space including the Re–Re σ, π, and δ orbitals along with their antibonding counterparts [53] indicated that the lead $\sigma^2\pi^4\delta^2\delta^{*0}\pi^{*0}\sigma^{*0}$ configuration makes up only ~63% of the total wavefunction. This conclusion is consistent with the symmetry breaking apparent in DFT-based studies of the same system [54, 55]. More recently, (8,8) and (12,12) active spaces (the latter including the Re–Cl σ and σ* orbitals) have been used to optimize the geometry of $[Re_2Cl_8]^{2-}$, the resulting Re–Re bond length being in good agreement with X-ray data [56, 57]. The occupations of the δ and δ* orbitals in the CASSCF wavefunction (~1.5 and ~0.5, respectively) confirm the weakness of the δ bond.

While $[Re_2Cl_8]^{2-}$ is certainly the iconic quadruply bonded molecule, a number of isoelectronic analogs have also been reported including the rhenium bromide [58] and iodide [59], as well as the lighter $[Tc_2X_8]^{2-}$ congeners (X = Cl, Br) [60] and the group VI tetraanions $[Mo_2X_8]^{4-}$ and $[W_2X_8]^{4-}$ [61]. In the osmium analogs, $[Os_2X_8]^{2-}$ (X = Cl, Br), where the presence of two additional electrons in the δ* orbital [62, 63] annihilate the δ bond, the OsX_4 units adopt the more sterically favored staggered conformation. The weakness of the δ component of the metal–metal bond also gives rise to somewhat counterintuitive structural changes upon one-electron reduction of $[Tc_2Cl_8]^{2-}$. Both $[Tc_2Cl_8]^{2-}$ (formal bond order 4.0) and $[Tc_2Cl_8]^{3-}$ (formal bond order 3.5) have been structurally